Journal of Applied Polymer Science

Char Barrier Effect of Graphene Nanoplatelets on the Flame Retardancy and Thermal Stability of High-Density Polyethylene Flame-Retarded by Brominated Polystyrene

Shiya Ran,[1] Chao Chen,[1] Zhenghong Guo,[2] Zhengping Fang[1,2]

[1]MOE Key Laboratory of Macromolecular Synthesis and Functionalization, Institute of Polymer Composites, Zhejiang University, Hangzhou 310027, China

[2]Laboratory of Polymer Materials and Engineering, Ningbo Institute of Technology, Zhejiang University, Ningbo 315100, China

Correspondence to: Z. Guo (E-mail: guozhenghong@nit.zju.edu.cn)

ABSTRACT: Graphene nanoplatelets (GNPs) with the char barrier effect were combined with brominated polystyrene (BPS) and antimony trioxide (Sb_2O_3) to improve the flame retardancy and thermal stability of high-density polyethylene. Thermogravimetric analysis, limited oxygen index (LOI) testing, and vertical burning testing (UL-94) showed that the presence of GNPs led to enhanced thermal oxidation stability and significantly reduced the flammability. The addition of 1 wt % GNPs to polyethylene/BPS–Sb (mass ratio = 92/6/2) led to UL-94 grades from NG (first burning time > 30 s) to V-2 (total burning time = 14 s), and the LOI value increased from 23.4 to 24.1%. The results of the pyrolysis products provided evidence that the GNPs restricted volatilization. The morphology of the chars also proved the formation of the char layer, which could act as a barrier to isolate the material from the flame and retard the vaporization of flammable gases via a tortuous pathway. © 2014 Wiley Periodicals, Inc. J. Appl. Polym. Sci. **2014**, *131*, 40520.

KEYWORDS: composites; flame retardance; graphene and fullerenes; nanotubes; polyolefins; thermal properties

Received 5 December 2013; accepted 30 January 2014

DOI: 10.1002/app.40520

INTRODUCTION

High-density polyethylene (HDPE) is one of the most widely used polyolefins because of its balanced mechanical properties, chemical resistance, and ease of processing. However, its inherent flammability has limited its applications in some fields where excellent flame retardancy is required.[1,2] To reduce the flammability of HDPE, various flame-retardant additives have been developed. Halogen-containing compounds, which are known for their effective gas-phase flame inhibition mechanism, have been reported to be the most common flame retardant for HDPE because of their excellent fire resistance.[3,4] Moreover, some kinds of environmentally friendly brominated flame retardants have been commercialized that do not produce dioxin during burning.

There have been numerous attempts[5–11] to combine nanoparticles, such as clay and carbon nanotubes, with halogenated conventional flame-retardant additives to overcome the limitation of traditional flame retardants, such as the required high loading. It is believed that nanoparticle incorporation can be synergistic with brominated flame retardants via an effective barrier mechanism to impede the transfer of volatile products from the interior of polymer matrix and prevent heat transfer.[12–15]

Graphene nanoplatelets (GNPs) are stacks of multilayered graphene sheets and have attracted tremendous attention in recent years. GNPs have been incorporated with different polymers to gain outstanding performances in mechanical, thermal, electrical, optical, and barrier properties.[16,17] Because of their structure of nanometer-scaled thickness similar to other nanosheets, even GNPs with low loading levels can lead to effective barrier properties through the inhibition of flow of flammable gases, which results in efficient condensed-phase flame retardancy.

Although synergistic effects between brominated flame retardants and some kinds of nanoparticles have been reported, limited work has been done to investigate how GNPs influence the fire properties of brominated flame-retardant polymers. GNPs were introduced into this system to reduce smoke and heat productivity and to lead to improved flame retardancy. In light of the preceding discussion, we first discuss the effect of the GNPs and brominated polystyrene (BPS) on the flame retardancy of HDPE.

EXPERIMENTAL

Materials

HDPE (code 5000S, MFR (melt flow rate) = 0.9 g/10 min) was purchased from Yangzi Petrochemical Co., Ltd. (Nanjing,

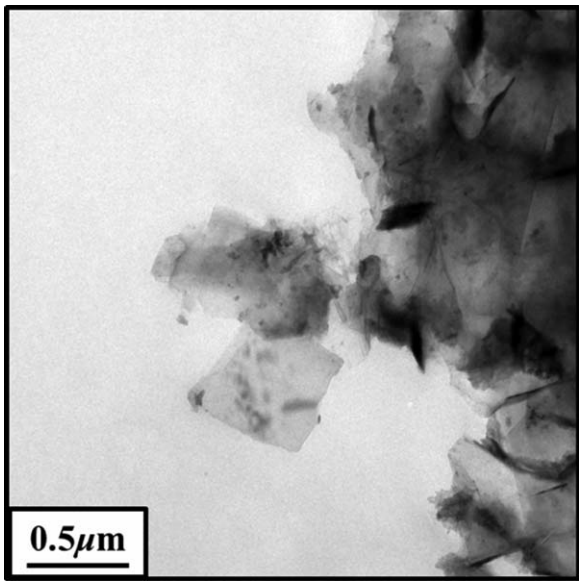

Figure 1. TEM image of the GNPs.

China). BPS (code SAYTEX-3010, theoretical bromine content ≈ 68.5%) was purchased from Albemarle Co. Antimony trioxide (Sb_2O_3) was purchased from No. 4 Reagent & H. V. Chemical Co., Ltd. (Shanghai, China). The GNPs (code KNG-150) were obtained from Xiamen Knano Graphene Technology Co., Ltd. (Xiamen, China). The GNPs were stacks of multilayered graphene sheets having a platelet morphology (as shown in Figure 1). The carbon content was greater than 99.5%, and the density was about 2.25 g/cm^3.

Preparation of the Flame-Retardant HDPE Composites

The brominated flame-retardant HDPE composites were melt compounded with a Thermo Haake Rheomixer (Typ557-8310, Germany) at 200°C for 8 min at a rotor speed of 60 rpm. The Sb_2O_3 and GNPs were premixed with BPS first and then composed with HDPE. The prepared composites were transferred into a mold, preheated for 5 min at 200°C, and then pressed at 15 MPa for 8 min; this was followed by pressing at room temperature under the same pressure for 5 min. The formulations are listed in Table I.

Characterization

The transmission electron micrographs (JEOL, Japan) were obtained with a JEM-1200EX electron microscope at an accelerating voltage of 120 kV. Thermogravimetric analysis (TGA) was performed on a TGA 209 F1 (Netzsch, Germany) at a heating rate of 20°C/min in an air atmosphere from 30 to 700°C. TGA–Fourier transform infrared (FTIR) measurements were carried out with a TGA 209 F1 instrument (Netzsch) coupled with a Thermo Nicolet iS10 FTIR spectroscope (Thermo-Fisher, Germany). The temperature program was the same as that used for TGA, and the sample mass was fixed at 6.0 mg. Limited oxygen index (LOI) values were determined with an HC-2 oxygen index instrument (Jiangning, China) according to ASTM D 2863 with the sample dimensions of 150 × 6 × 3 mm^3. UL-94 tests were measured on a CZF-2 instrument (Jiangning, China) according to ASTM D 3801 with sample dimensions of 130 × 13 × 3 mm^3. Scanning electron microscopy (SEM) observation of the char residues was carried out on an S-4800 microscope (TSM-5510, Japan) under an accelerating voltage of 3 kV. Samples with dimensions of 15 × 6 × 3 mm^3 used for the analysis of morphology for the residual chars were placed in a muffle furnace at 400°C for 5 min.

Table I. Formulations of the Brominated Flame-Retardant HDPE Composites

Sample	HDPE	BPS	Sb_2O_3	GNPs
PE	100	0	0	0
PE/BPS–Sb	92	6	2	0
PE/BPS–Sb/GNPs	92	6	2	1

The values are weight fractions.

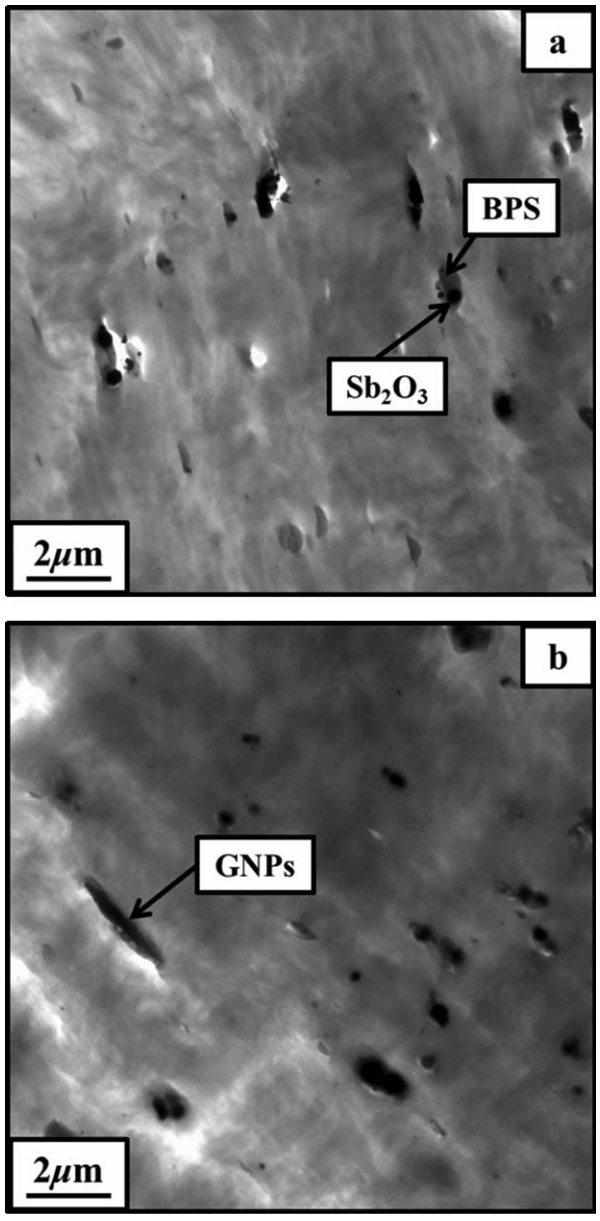

Figure 2. TEM images of the (a) PE/BPS–Sb and (b) PE/BPS–Sb/GNP composites.

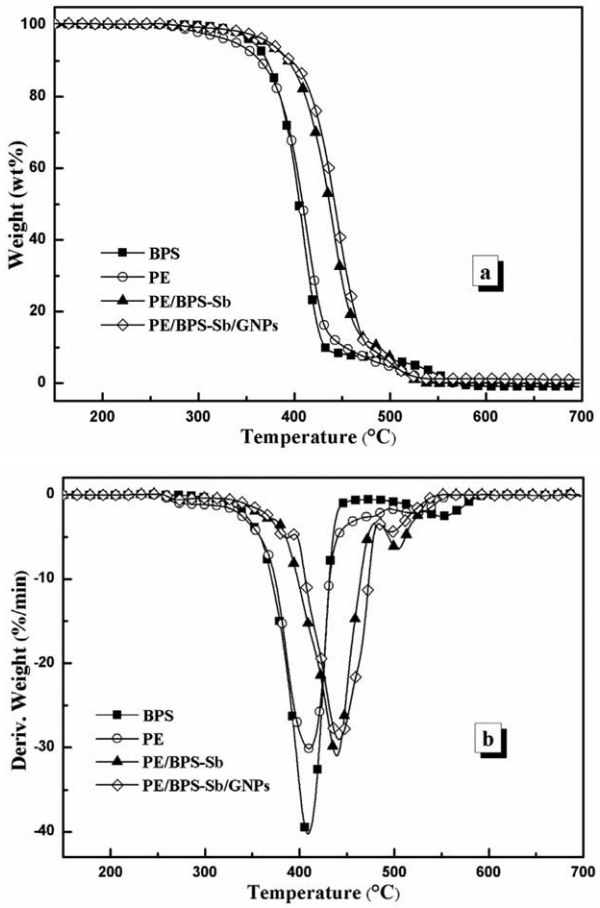

Figure 3. (a) TGA and (b) DTG curves of the BPS and flame-retardant composites in air.

RESULTS AND DISCUSSION

Morphology

Figure 2 contains the TEM micrographs of the polyethylene (PE)/BPS–Sb and PE/BPS–Sb/GNP composites. Because of the poor compatibility between the HDPE and BPS/Sb_2O_3 components, a typical matrix–droplet structure was observed, and Sb_2O_3 adheres to BPS phase due to the strong polarity of BPS. As shown in Figure 2(a), the droplets (1–2 μm) of BPS gathering with Sb_2O_3 presented as dark areas, and no severe aggregation of discrete phases was observed. After the addition of GNPs, the orientation caused by the melt shear force became clear, and the GNPs converged with the BPS/Sb_2O_3 with dimensions of about 1–2 μm, as presented in Figure 2(b). It seemed that the addition of GNPs had little effect on the dispersive states of BPS and Sb_2O_3.

The thermal oxidation degradation of the PE, PE/BPS–Sb, and PE/BPS–Sb/GNP composites were tested by TGA, and the TGA and DTG (Derivative TG) curves in an air atmosphere are shown in Figure 3, with the detailed data listed in Table II. Under an air atmosphere, HDPE experienced a rapid thermal oxidation decomposition accompanied by hydrogen abstraction.[18] The onset decomposition temperature [herein defined as the temperature at which 5 wt % degradation occurs ($T_{5\%}$)] for neat HDPE was around 339°C, and its TGA trace showed two weight loss stages, with the maximum decomposition temperatures

Table II. Data from the TGA and DTG Curves for the BPS and Flame-Retardant Composites in Air

Sample	$T_{5\%}$ (°C)	$T_{50\%}$ (°C)	T_{max1} (°C)	T_{max2} (°C)	Residue at 600°C (wt %)
BPS	358	409	409	550	0
PE	339	409	410	522	0
PE/BPS-Sb	368	436	442	503	0.1
PE/BPS-Sb/GNPs	372	442	444	496	1.4

(T_{max}, the temperature at the rate of maximum decomposition) at 410 and 522°C. The first decomposition step was the oxidation of HDPE, and the second step may have been the decomposition of the products formed by the oxidation of HDPE.[19,20] Also, pure HDPE at 700°C did not produce any char residue. For the PE/BPS–Sb composites, the presence of brominated flame retardant remarkably improved the thermal oxidation decomposition of HDPE. The brominated flame retardant in free-radical trapping caused the $T_{5\%}$, $T_{50\%}$ [herein defined as the temperature at which 50 wt % degradation occurs ($T_{50\%}$)], and T_{max1} values to increase by about 30°C.

Moreover, in the PE/BPS–Sb/GNPs, $T_{5\%}$ increased from 368 to 372°C and $T_{50\%}$ increased from 436 to 442°C compared with the PE/BPS–Sb composite. At the same time, an increase in char formation was present. The improvement in the thermal oxidation stability might have been due to the physical protective barrier of GNPs in the HDPE matrix, which retarded the permeation of flame and the escape of volatile degradation products via a tortuous pathway. Hence, the addition of GNPs was beneficial to the improvement of the thermal oxidation stability of the PE/BPS–Sb composite.

Flammability

As simple and important methods for evaluating the flame retardancy of polymeric materials, vertical flame testing and LOI testing were conducted to understand the combustion behavior of the brominated flame-retardant HDPE composites, and the results are presented in Table III. Pure HDPE exhibited an LOI value of 16.5% and was highly combustible; it showed no classification in the UL-94 test. When 8 wt % BPS–Sb was added, the LOI value went to 23.4%, but this composite still failed in the vertical burning test. When 1 wt % GNPs were

Table III. Flame Retardancy of the Flame-Retardant HDPE Composites

Sample	Total burning time: $t_1 + t_2$ (s)[a]	UL-94 grade	LOI (% O_2)
PE	$t_1 > 30$	NG[b]	16.5
PE/BPS-Sb	$t_1 > 30$	NG[b]	23.4
PE/BPS-Sb/GNPs	14	V-2	24.1

[a] A flame was applied to each sample for 10 s and removed. The time that the sample continued to burn was recorded as t_1. The flame was then reapplied for another 10 s, and the burning time after removal was recorded as t_2.
[b] NG, no grading and burned up to the upper clamp at the stand.

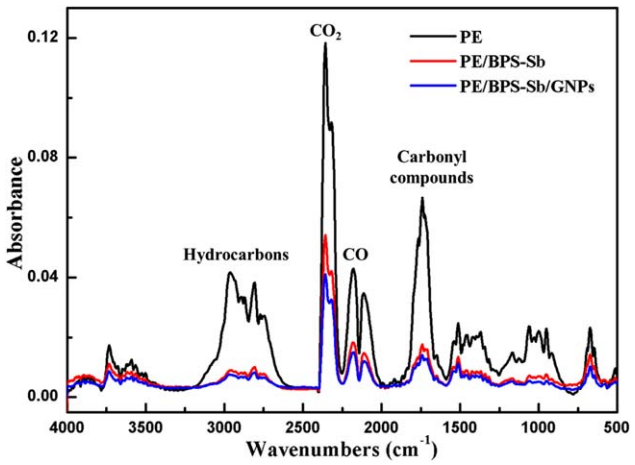

Figure 4. FTIR spectra of the flame-retardant HDPE composites at the maximum evolution rate. [Color figure can be viewed in the online issue, which is available at wileyonlinelibrary.com.]

incorporated, the LOI value was higher than that with BPS–Sb alone. Furthermore, PE/BPS–Sb/GNPs reached the UL-94 V-2 grade and showed lower times of burning. The improvements in the flame retardancy almost matched what was observed for the thermal oxidation properties. Similar results have also been found in previous graphene-based and clay-based nanocomposites.[6,7,21,22] The gas-phase flame-retardant mechanism of BPS was combined with the condensed phase of the GNPs, which enhanced the flame retardancy of the brominated flame-retardant composites.

Volatilized Products of the Flame-Retarded HDPE Composites Analyzed by TGA–FTIR Spectroscopy

The TGA–FTIR technique can give information about pyrolysis products, which provides insight into thermal degradation mechanisms.[21] Figure 4 presents the relative intensity of the absorption peaks of the PE, PE/BPS–Sb, and PE/BPS–Sb/GNP composites at temperatures above 409°C, that is, T_{max} of HDPE in air. Some small molecular gaseous decomposition products of pure HDPE were identified unambiguously by the characteristic strong bands of hydrocarbons (2950–2800 cm^{-1}), CO_2 (2355 cm^{-1}), CO (2180 cm^{-1}), and carbonyl-containing compounds (1745 cm^{-1}). The FTIR spectra of the brominated flame-retardant composites exhibited the similar gaseous products as that of pure HDPE. However, the intensity of the gas emissions of the PE/BPS–Sb and PE/BPS–Sb/GNP composites were much lower than that of pure PE, whereas the lowest intensity was observed for the PE/BPS–Sb/GNPs composite. This suggested that the amount of volatile compounds generated by thermal oxidation was much lower for the brominated flame-retardant composites.

To further understand the change of the pyrolysis products for HDPE and its brominated flame-retardant composites, the absorbance of pyrolysis products versus time is revealed in Figure 5. The pyrolysis products for brominated flame-retardant composites started to release at about 17.5–18.0 min; this was later than that of pure HDPE (16.5 min). Also, the time of maximum release rate was about 22 min for the brominated flame-retardant composites and 20.5 min for HDPE. This was interpreted as being due to the chemical reaction between BPS and Sb_2O_3 to generate gas-phase flame retardance. At the same

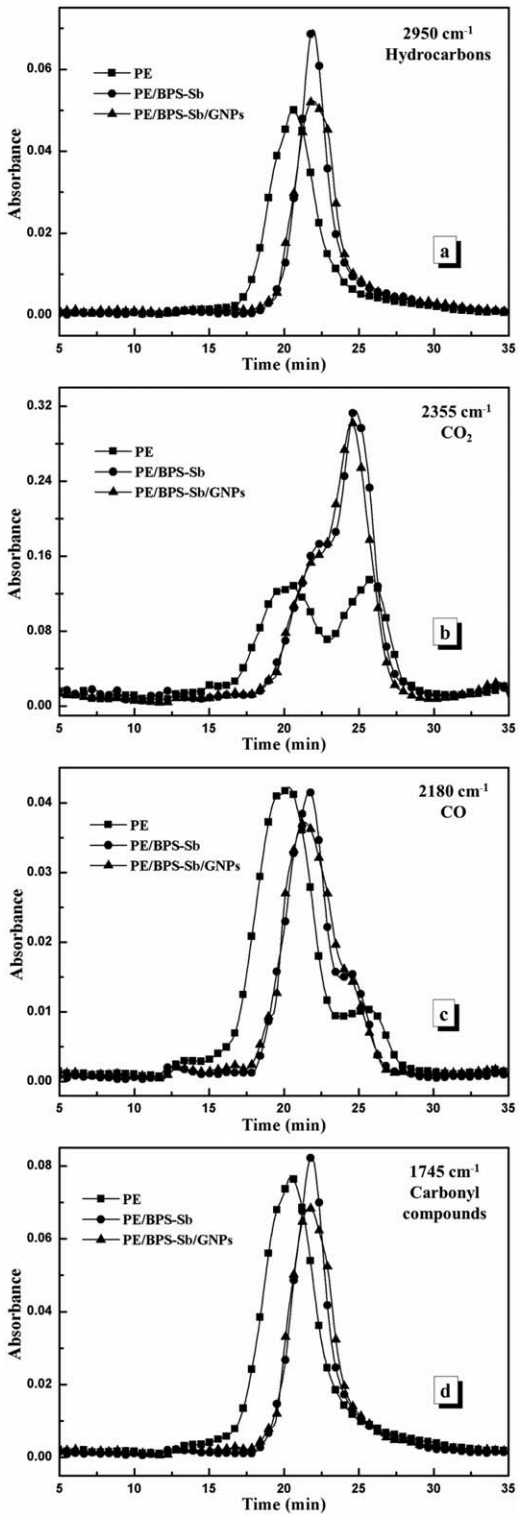

Figure 5. Absorbance of pyrolysis products for the flame-retardant HDPE composites versus time: (a) hydrocarbons, (b) CO_2, (c) CO, and (d) carbonyl compounds.

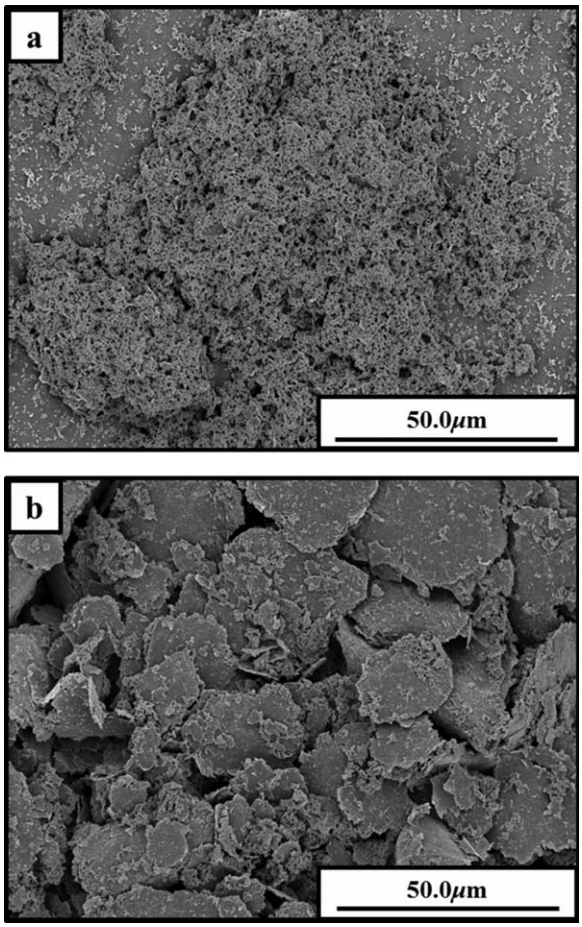

Figure 6. SEM images of the outer surface of char: (a) PE/BPS–Sb and (b) PE/BPS–Sb/GNP composites.

time, the absorbent intensity of the pyrolysis products for the PE/BPS–Sb/GNPs composite was lower than that of the PE/BPS–Sb composite, including hydrocarbons, carbonyl compounds, and CO, which agreed well with Figure 5. It is worth noting that the reduction of CO gave rise to a decrease in the toxicity of the gaseous products during combustion.[22] The GNPs acted as a barrier to prevent the combustible gases from transferring to the surface of the materials and feeding the flame. Meanwhile, the release of nonflammable gases (e.g., CO_2) diluted the combustible gas and thus retarded the combustion.

Analysis of the Char Residue

To further investigate the effect of the GNPs on the char formation of the brominated flame-retardant composites during combustion, the morphology of the chars was examined by SEM. Figure 6 presents the SEM graphs of the char layer from the combustion of the PE/BPS–Sb and PE/BPS–Sb/GNP composites at 400°C in the muffle furnace for 5 min. As shown in Figure 6(a), the PE/BPS–Sb composite has been burned completely only with a few porous chars left. However, the char layers of the PE/BPS–Sb/GNPs composite, as shown in Figure 6(b), appeared to have a compact and layered structure. The GNPs could have been acted as a physical protective barrier to block the transfer of mass and heat between the gas and condensed phase; this also contributed to a reduction in the flammability of the polymer materials to some degree.

CONCLUSIONS

The thermal and flammability performance of the brominated flame-retardant HDPE composites with GNPs was investigated. The assembly of the BPS–Sb and GNPs afforded good flame retardancy in the HDPE matrix compared with that of the BPS–Sb alone. After the addition of the GNPs, the UL-94 V-2 grade was obtained with a higher LOI value of 24.1%; this indicated that there existed combined effects from the GNPs and BPS. TGA–FTIR spectroscopy and residual analysis by SEM revealed that the improvement in the flame retardancy was especially attributed to the tortuous pathway effects of the GNPs. In this manner, the evolution of the degradation products was slowed down; this increased the effectiveness of radical entrapment in the gas phase. Accordingly, we concluded that the hot radical entrapment by BPS in the gas phase was coupled with the physical char barrier action of the GNPs in the condensed phase. This increased the overall flame-retardant effectiveness.

ACKNOWLEDGMENTS

This work was financially supported by the National Natural Science Foundation of China (contract grant number 51203137), the Zhejiang Provincial Natural Science Foundation (contract grant number LY12E03003), and the Ningbo City Natural Science Foundation (contract grant number 2011A610124).

REFERENCES

1. Tsai, K. C.; Kuan, H. C.; Chou, H. W.; Kuan, C. F.; Chen, C. H.; Chiang, C. L. *J. Polym. Res.* **2011**, *18*, 483.
2. Lee, Y. H.; Kuboki, T.; Park, C. B.; Sain, M.; Kontopoulou, M. *J. Appl. Polym. Sci.* **2011**, *118*, 452.
3. Cusack, P. A.; Heer, M. S.; Monk, A. W. *Polym. Degrad. Stab.* **1997**, *58*, 229.
4. Giúdice, C. A.; Benítez, J. C. *Prog. Org. Coat.* **2001**, *42*, 82.
5. Zanetti, M.; Camino, G.; Canavese, D.; Morgan, A. B.; Lamelas, F. J.; Wilkie, C. A. *Chem. Mater.* **2002**, *14*, 189.
6. Chen, X. S.; Yu, Z. Z.; Liu, W.; Zhang, S. *Polym. Degrad. Stab.* **2009**, *94*, 1520.
7. Chen, Y. J.; Guo, Z. H.; Fang, Z. P. *Polym. Eng. Sci.* **2012**, *52*, 390.
8. Zhuo, D. X.; Wang, R.; Wu, L. X.; Guo, Y. H.; Ma, L.; Weng, Z. X.; Qi, J. Y. *J. Nanomater.* **2013**, DOI: 10.1155/2013/820901.
9. Wang, C. Q.; Ge, F. Y.; Sun, J.; Cai, Z. S. *J. Appl. Polym. Sci.* **2013**, *130*, 916.
10. Huang, G. B.; Chen, S. Q.; Tang, S. W.; Gao, J. R. *Mater. Chem. Phys.* **2012**, *135*, 938.
11. Liu, X. S.; Gu, X. Y.; Zhang, S.; Jiang, Y.; Sun, J.; Dong, M. Z. *J. Appl. Polym. Sci.* **2013**, *130*, 3645.
12. Lu, H. D.; Wilkie, C. A. *Polym. Degrad. Stab.* **2010**, *95*, 564.

13. Lewin, M.; Zhang, J.; Pearce, E.; Zammarano, M. *Polym. Adv. Technol.* **2010**, *21*, 825.
14. Ozkaraca, A. C.; Kaynak, C. *Polym. Compos.* **2012**, *33*, 420.
15. Hapuarachchi, T. D.; Peijs, T.; Bilotti, E. *Polym. Adv. Technol.* **2013**, *24*, 331.
16. Terrones, M.; Botello-Méndez, A. R.; Campos-Delgado, J.; López-Urías, F.; Vega-Cantú, Y. I.; Rodríguez-Macías, F. J.; Elías, A. L.; Muñoz-Sandoval, E.; Cano-Márquez, A. G.; Charlier, J. C.; Terrones, H. *Nano Today* **2010**, *5*, 351.
17. Goosey, M. *Circuit World* **2012**, *38*, 83.
18. Zanetti, M.; Camino, G.; Reichert, P.; Mülhaupt, R. *Macromol. Rapid Commun.* **2001**, *22*, 176.
19. Wu, G.; Song, Y. H.; Zheng, Q.; Du, M.; Zhang, P. J. *J. Appl. Polym. Sci.* **2003**, *88*, 2160.
20. Zhao, L. P.; Song, P. A.; Cao, Z. H.; Fang, Z. P.; Guo, Z. H. *J. Nanomater.* **2012**, DOI: 10.1155/2012/340962.
21. Wang, X.; Hu, Y.; Song, L.; Yang, H. Y.; Yu, B.; Kandola, B.; Deli, D. *Thermochim. Acta* **2012**, *543*, 156.
22. Wang, X.; Song, L.; Yang, H. Y.; Xing, W. Y.; Lu, H. D.; Hu, Y. *J. Mater. Chem.* **2012**, *22*, 3426.